Proceedings of National Conference on CFD Applications in Power & Industry Sectors, at Corporate (R&D) Division, BHEL, Hyderabad-500 093, India, Nov 17-18, 2006

Use of CFD Methods for Aerodynamic Analysis of Wind Turbine Blades

Krishna Murthy S. J.*, K. R. Srilatha* and Kishor Kumar**
National Aerospace Laboratories, Bangalore-560 017.
Email: sjkmurthy@webmail.nal.res.in
* Scientist, NAL, Bangalore.
** Lecturer, Vemana Institute of Technology, Bangalore

Aerodynamic analysis & performance evaluation of a 300 kW stall-regulated Horizontal Axis Wind Turbine Blades is carried out using commercially available computer code 'GH Bladed' Version 3.6 provided by Centre for Wind Energy Technology, Chennai and Wind Turbine Performance Evaluation Program of NAL. Effort has been made to use in-house developed Implicit 2-D Reynolds Averaged Navier-Stokes code validated for several airfoils in characterizing the blade profiles. Post- Stall characteristics of airfoils are derived values from Garrad Hassan report. Time averaged field measured power output shows good agreement with the computed results from GH-Bladed as well as Wind Turbine Evaluation Program over a range of wind speeds.

1. Introduction

National Aerospace Laboratories (NAL) has a major project on development of cost effective medium scale wind turbine suitable for Indian conditions for harnessing renewable energy from the nature, sponsored by CSIR under New Millennium Indian Technology Leadership Initiative (NMITLI). The annual average wind speed in India is very close to 6.5-7.0 m/s. The design of optimum, cost effective as well as maximum annual energy extraction using wind turbines is a challenging task. Airfoils designed and generated for aeroplane wings were earlier used in wind turbines. CFD methods developed for aerospace applications find extensive utility in generation of design data and analysis of wind turbines. In-house developed Implicit 2-D Reynolds Averaged Navier - Stokes (IMPRANS) code has been validated for several airfoils in characterizing the blade profiles[1]. This is the first time an effort is made to use this code for wind turbine blade profiles in NAL.

The present analysis is based on the work carried out on a constant speed, fixed pitch, two bladed, down wind 300kW stall regulated horizontal axis wind turbine of M/s Sangeeth group of Companies, Kethanur, Coimbatore district. A test platform provided by M/s Sangeeth group of companies will be used to get the experimental results. Structural design, fabrication and structural testing of two blades had been completed at NAL. Field testing is in progress at M/s Sangeeth wind farms. This became necessary in view of sustained technology support and state of art technology requirements sought by M/s Sangeeth group of companies.

This paper presents comparative study of airfoils characteristics of wind turbine blades computed using 2-D IMPRANS code and wind tunnel measurements made on low speed airfoils of different thickness ratios at NASA[2,3,4]. Also presents the application of a simple and most widely used Wind Turbine Performance Evaluation Program (WTPE-BEMT) based on blade element momentum theory [5] and commercially available software package for wind turbine performance and loading calculations by Garrad Hassan 'GH Bladed' Version 3.6 [6] provided by Centre for Wind Energy Technology, Chennai for evaluating constant speed, fixed pitch 300 kW stall-regulated horizontal axis wind turbines (HAWT). The time averaged field measurement of power output carried out by National Aerospace Laboratories [7] were compared with the computed results.

2. Airfoil geometry

The Sangeeth Wind Turbine (SWT) blade geometric parameters have been evaluated by measuring the blade dimensions [8]. The blade chord, thickness distribution and twist are shown in the figures 2.1,2.2 & 2.3. The measured profiles were compared with the low speed (LS) profiles of aircraft wings. Figure 2.4 shows the profile measured and LS (1)-modified. Though the profiles are close to the LS (1)-0413-modified, measured profiles show slightly higher thickness near the trailing edges. Maximum thickness, chord and twist show good agreement with similar work carried out by D.C. Quarton et al,. [9].

3. Characterization of Airfoil Sections Using N-S Code

The Implicit Two-dimensional Reynolds Averaged Navier-Stokes solver for compressible viscous flow around airfoils (IMPRANS) [1] developed at CTFD Division of NAL is used to characterize the airfoils. The solver is based on an implicit finite volume nodal point scheme wherein a control volume is formed by joining the centroids of the neighboring cells around the nodal point in the computational domain.

1) Governing equations:

The two-dimensional Navier-strokes equations for unsteady viscous compressible flow can be written in non-dimensional conservative form [1]

$$\frac{\partial U}{\partial t}+\frac{\partial F}{\partial x}+\frac{\partial G}{\partial y}=\frac{\partial V}{\partial x}+\frac{\partial W}{\partial y} \qquad (1)$$

Where x and y are Cartesian coordinates and t – time variable, U vector of conserved variables and F, G, V, W are the flux vectors.

$$U=\begin{bmatrix}\rho\\ \rho u\\ \rho v\\ e\end{bmatrix}, F=\begin{bmatrix}\rho u\\ \rho u^2+p\\ \rho uv\\ (e+p)u\end{bmatrix}, G=\begin{bmatrix}\rho v\\ \rho uv\\ \rho v^2-p\\ (e+p)v\end{bmatrix} \qquad (2)$$

The primitive variables are density ρ, velocity components u, v in x and y directions, pressure p, temperature T and total energy per unit volume e.

$$V = V_1(U, U_x) + V_2(U, U_y)$$

$$V=\frac{1}{\mathrm{Re}_\infty}\begin{bmatrix}0\\ \lambda(u_x+v_y)+2\mu u_x\\ \mu(v_x+u_y)\\ \mu\beta(u_y+v_x)+\lambda\beta(u_x+v_y)+2\mu\beta u_x+\dfrac{\mu\beta T_x}{(\gamma-1)M_\infty^2 P_r}\end{bmatrix} \qquad (3)$$

$$W = W_1(U, U_x) + W_2(U, U_y)$$

$$W=\frac{1}{\mathrm{Re}_\infty}\begin{bmatrix}0\\ \mu(u_y+v_x)\\ \lambda(u_x+v_y)+2\mu v_y\\ \mu\beta(u_y+v_x)+\lambda\beta(u_x+v_y)+2\mu\beta v_y+\dfrac{\mu\beta T_y}{(\gamma-1)M_\infty^2 P_r}\end{bmatrix} \qquad (4)$$

The inviscid flux vectors F and G are functions of U alone while the flux vectors V and W contain viscous terms which are functions of U, U_x and U_y. M_∞ and Re_∞ are the free stream Mach number and Reynolds number respectively. γ is the ratio of specific heats, λ and μ are viscosity coefficients and Pr is the prandtl number. The non-dimensional variables used in the above equation has been obtained by using the following free stream values as reference quantities: ρ_∞ (Density), U_∞ (Velocity), l (length), μ_∞ (Viscosity), T_∞ (Temperature), $\rho_\infty U_\infty^2$ (Pressure) and so on. Finally the system is closed using the perfect gas equation of state in non-dimensional form as

$$p = \frac{\rho T}{\gamma M_\infty^2} \qquad (5)$$

2) Finite volume formulation:

Applying the Eulers implicit time differencing formula [1]

$$U^n = U^{n+1} - \left(\frac{\partial U}{\partial t}\right)^{n+1}\Delta t + O(\Delta t^2) \qquad (6)$$

To the governing equations (1), we obtain

$$\Delta U^n + \Delta t\left[\frac{\partial}{\partial x}(F-V)+\frac{\partial}{\partial y}(G-W)\right]^{n+1} = 0 \qquad (7)$$

Here $U^n = U(t) = U(n\Delta t)$ is the solution vector at time level n and $\Delta U^n = (U^{n+1} - U^n)$ is the change in U_n over the time step Δt. In order to facilitate the finite volume formulation, the above equations are written in the integral form as

$$\iint_\Omega \Delta U^n dx dy + \Delta t\int_\Gamma [(F-V)^{n+1}dy-(G-W)^{n+1}dx] = 0 \qquad (8)$$

Where Ω is any two dimensional flow domain and Γ is the boundary curve. In the nodal point finite volume approach [1], the flow variables are associated with each mesh point of the grid and the interval conservative equations are applied to each control volume obtained by joining the centroids of the four neighbouring cells of a nodal point. The following figure shows a typical control volume Ω_{ij} formed by joining the centers a, b, c, d of the four cells surrounding a nodal point (i,j) of a body fitted curvilinear grid, i, j being the spatial indices along curvilinear coordinate directions ξ, η. By discretizing the equation (8) and linearising the inviscid flux vector expanding with time using Taylor series as well as discretizing viscous flux vectors in the physical plane, then solution is obtained. The following equations for computational cells Ω_{ij}.

$$\Delta U_{ij}^n h_{ij} + \Delta t\int[(F-V)^{n+1}dy-(G-W)^{n+1}dx] = 0 \qquad (9)$$

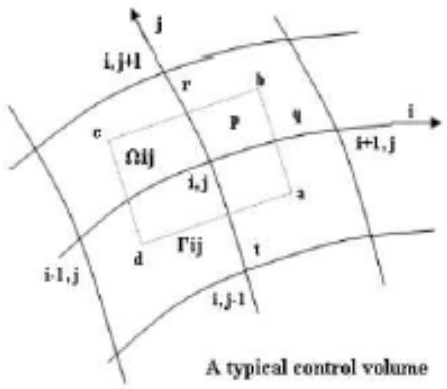

A typical control volume

Where h_{ij} is the area of quadrilateral abcd and the integral refers to a contour integration around the boundary Γ_{ij} of the cell Ω_{ij} taken in anticlockwise direction. The fluxes are to be calculated across the four sides of the control volume abcd. Convergence is obtained by adding the artificial dissipation form to the conservative variables. C-type grids were used to compute both laminar and turbulent flows around airfoil. Turbulence closure was achieved by employing the algebraic eddy viscosity model of Baldwin and Lomax. The solver has been validated extensively for steady compressible flow past a variety of airfoils such as NACA0012, RAE 2822, GAW (2) and helicopter blade profiles. This is the first time an effort is made to use this code for wind turbine blade profiles in NAL. This code is being used to characterize the airfoil sections for lift, drag and moment coefficients over a range of operating Mach numbers, angle of attack and the operating Reynolds numbers. N-S computed values have been compared with the wind tunnel data for different thickness ratios of blade profiles [2,3,4]. Figure 3.1 to 3.3 shows the comparison between the IMPRANS results and that of NASA wind tunnel measurements for thickness ratios of 13%,17% and 21%. It is observed from the figures that the coefficients of lift and drag in the attached flow regime is in good agreement with the tunnel measurements. For thickness ratio of 13% the C_{lmax} is slightly lower and corresponding C_d is slightly higher than the measured values at Reynolds number $2x10^6$. In the stall and post stall regime, code predicted stall angle is lower by 2 degrees and higher drag coefficient than tunnel-measured values. For the thickness ratios of 17% and 21% computed C_{lmax} and C_d is slightly higher at proximity to stall and, in the stall and post stall regimes computed coefficients of lift, drag and stall angle are higher than the tunnel-measured values. In view of the above discrepancies, derived coefficients of lift and drag in the stall and post stall regimes are from report[9] with post stall correction of flat plate theory is used in computing the performance of the wind turbine.

4. Performance Evaluation of wind turbine

a) Wind Turbine Performance Evaluation -Blade Element Momentum Theory Combined blade element and momentum theory is an extension of the actuator disk theory. The basic assumption of the BEMT is that the force of a blade element is solely responsible for the change of momentum of the air, which passes through the annulus swept by the element. It is therefore to be assumed that there is no radial interaction between the flows through contiguous annuli-a condition that is, strictly, only true if the axial flow induction factor does not vary radially. The rotor blades are divided into a number of blade elements and a series of annuli swept out by each blade element and where each annulus is assumed to act in the same way as an independent actuator disc. At each radial position the rate of change of axial momentum and angular momentum are equated with the thrust and torque produced by each blade element.Figure 4.1 shows the velocity triangle and force diagram of a wind turbine blade.

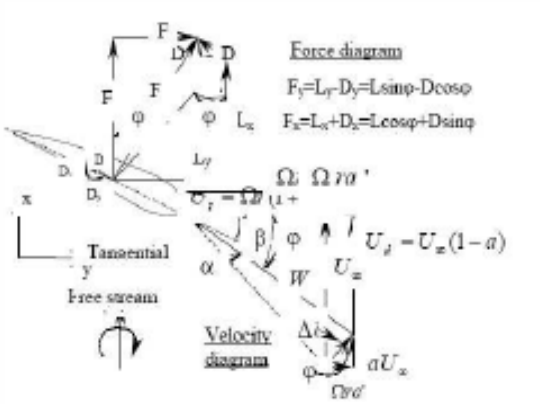

Fig 4.1 Velocity and Force diagram of wind turbine rotor disc(coned)

The resultant relative inflow velocity of blade is

$$W=\sqrt{(U_\infty^2(1-a)^2+\Omega^2r^2(1+a')^2)}$$

which acts at an angle Φ to the plane of rotation, such that

$$\sin\phi=\frac{U_\infty(1-a)}{W}\ and\ \cos\phi=\frac{\Omega r(1+a')}{W}$$

Here a is axial inflow factor, a' is tangential inflow factor, Ω is angular velocity and U_∞ is free stream wind velocity.
The angle of attack is given by

$$\alpha=\phi-\beta$$

Where α is angle of attack in deg, Φ is relative inflow angle and β is twist angle of blade. The lift and drag forces on a span-wise length δr of blade, normal and parallel to the direction of W respectively,

$$\delta L = \frac{1}{2}\rho W^2 c C_l \delta r\,;\ \delta D = \frac{1}{2}\rho W^2 c C_d r \delta r\,;$$

Here c is chord, ρ is density of the air, W is relative inflow velocity of air, Cl, Cd are lift and drag coefficients, r is local radius. The component of aerodynamic force on N elements resolved in axial direction is

$$\delta L\cos\phi + \delta D\sin\phi = \frac{1}{2}\rho W^2 Nc(C_l\cos\phi + C_d\sin\phi)\delta r;$$

here Φ is relative inflow angle. The rate of change in angular momentum of the air passing through annulus is

$$\rho U_\infty(1-a)\Omega r 2a' r 2\pi r\delta r = 4\pi\rho U_\infty(\Omega r)a'(1-a)r^2\delta r$$

U_∞ is free stream wind velocity. simplifying,

$$\frac{W^2}{U_\infty^2}N\frac{c}{R}(C_l\sin\phi - C_d\cos\phi) = 8\pi\lambda\mu^2 a'(1-a)$$

where $\mu = r/R$. it is convenient to put above equation in the following form

$$C_l\cos\phi + C_d\sin\phi = C_x \quad \text{and}$$
$$C_l\sin\phi - C_d\cos\phi = C_y$$

To obtain values of the flow induction factor a and a' using two-dimensional aerofoil characteristics requires an iterative process. The following equations which are convenient in the right-hand sides are evaluated using existing values of the flow induction factors yielding simple equations for the next iteration of the flow induction factors.

$$\frac{a}{1-a} = \frac{\sigma_r}{4\sin\phi^2}\left[C_x - \frac{\sigma_r}{4\sin^2\phi}C_y^2\right]$$

$$\frac{a}{1+a'} = \frac{\sigma_r C_y}{4\sin\phi\cos\phi}$$

The following equation gives the blade solidity which is a primary parameter in determining rotor performance.

$$\sigma_r = \frac{Nc}{2\pi r} = \frac{Nc}{2\pi\mu R};$$

Elemental thrust: $\frac{dT}{dr} = 4\pi\rho U_\infty^2 a(1-a)r\,;$

Elemental torque: $\frac{dQ}{dr} = 4\pi\rho U_\infty^3(\Omega r a')(1-a)r^2;$

Elemental power: $\frac{dP_a}{dr} = \Omega\left(\frac{dQ}{dr}\right);$

Total power, thrust and torque is obtained by integrating over the blade span. The coefficients of thrust power and torque of rotor at particular wind speed is calculated using,

$$C_T = \frac{T}{\frac{1}{2}\rho U_\infty^2\pi R^2}; \qquad C_P = \frac{P_a}{\frac{1}{2}\rho U_\infty^3\pi R^2};$$

$$C_Q = \frac{C_p}{\lambda};$$

Power:

$$P = C_p\times\frac{1}{2}\times\rho\times A_{eff}\times U^3\times\eta_g\times\eta_m;$$

η_g, η_m are electro-mechanical efficiencies.

The Tip-Loss factor is defined by the ratio between the bound circulation of all the blades and the circulation of a rotor with infinite number of blade. The prandtl tip-loss model is the most accepted correction employed in strip theory calculations of wind turbines. The tip loss factor F, which modifies the power output for the reduced circulation and blade unloading by tip-vortex shedding. Tip loss factors F(t) and F(h) for hub and tip respectively are ;

$$F(t) = \left(\frac{2}{\pi}\right)\left(\arccos\left(e^{f_t}\right)\right);\ \text{where } f_t = \left(\frac{B}{2}\right)\left(\frac{R_t - r}{r\sin\phi}\right);$$

$$F(h) = \left(\frac{2}{\pi}\right)\left(\arccos\left(e^{f_h}\right)\right);\ \text{where } f_h = \left(\frac{B}{2}\right)\left(\frac{r - R_h}{R_h\sin\phi}\right);$$

The hub-tip loss factor $F = F(t)xF(h)$; is used during iterative process of evaluating inflow factors a and a'

.Present analysis is based on the work carried out on constant speed, fixed pitch, two bladed, teetered hub, tilting tower, down wind 300kW stall regulated horizontal axis wind turbine of M/s Sangeeth Group of companies [10]. Wind turbine having tip diameter of 24m and hub diameter of 1.75m rotates at constant speed of 65rpm. It generates rated power of 300kW at a hub height wind speed of 19m/s. This turbine is mounted on a tilting tower of hub height 50m from the ground. Cut in and cut out wind speed is 4.5m/s and 34m/s respectively. Shaft tilt and pre cone angles are limited to 2 and 6 degrees

respectively. Shut down by pitching the blades to fully stalled condition. Coefficients of lift and drag of blade profiles, blade tip diameter, density of air, hub radius, blade twist at different ratio of chord to tip radius, ratio of hub radius to tip radius, wind shear exponent of 0.14 [11], pre-cone and shaft tilt were used to compute power, coefficients of power, torque and thrust at various free stream velocities of air using WTPE- BEMT program [5] for the prescribed speed of turbine rotor. Axial and tangential flow factors were arrived through iterative process. Prandtl loss model was incorporated in the program for calculating the hub and tip losses. Airscrew has been analyzed as wind turbine. In the post stall regime, flat plate model has been used in computing power output. Option to use NASA – Lewis synthesization routine is also possible. Efficiency is based on the inverse ratio of propeller model. Teetering hub design enables the turbine to avoid the gyroscopic loads inherent in a typical heavier three bladed turbines and also enables the turbines to quickly adjust to the changes in wind direction- free yaw with inertia damping. Teetering axis is perpendicular to shaft axis and located at the hinge point of the blades on the hub. Teetering is not considered in the present analysis. While computing, using the WTPE-BEMT program few selected (10) radial stations data were used. Elemental power, torque and thrust were computed and integrated over the blade span. The turbine operating range of Reynolds number is from 2 millions to 4 millions. In the present performance evaluation program, computation of power has been carried out using coefficients of lift and drag from IMPRANS for the attached flow regimes, stall and post stall data from report[2,3,4 & 9]. Empirical method as suggested by Viterna – Corrigan in evaluating the coefficients of lift and drag in the post stall regimes is not used in the present analysis. In a stall regulated, constant speed and fixed pitch wind turbine, wind turbine draws the power from the grid during very low speed of the wind to maintain the rotational speed. Hence cut-in wind speed is not very critical from the positive power production point of view but avoidance of drawing power from the grid is essential. Operation of wind turbines at close to stall is very important to get the maximum power output. Aerodynamic control system during stall is very essential to maintain the constant rotation speed and the power of the wind turbine. In view of the actual mechanical (gear box, etc) and electrical efficiencies are not easily available and also it change with the type of equipment we use, for preliminary analysis total efficiency of 80.36% is used. Figure 4.2 shows the Sangeeth wind turbine power varying with wind velocity computed up to 27.5m/s and also field measurements over a free stream air velocities varying from 4 m/s to 18.5m/s. Figure 4.3 shows coefficient of power at various tip speed ratios of Sangeeth wind turbine. Hub height from the ground is one of the parameter which could vary the power output of the turbine. WTPE-BEMT program allows hub height variation while computing the power output. Power output substantially increases with increase in air density.

b) Performance Evaluation using GH- Bladed

Performance evaluation is also carried out using software package "GH-Bladed" through C-WET [6]. "GH- Bladed" is a commercially available wind turbine performance and loading calculations tool provided by Garrad Hassan and Partners Limited. It has Graphical User Interface and can be used more comprehensively with any type of HAWTs. It is based on BEMT, and has many features. The induced axial and tangential flow factors may be determined using equilibrium, frozen or dynamic wake models. A tip loss model due to Prandtl and dynamic stall model due to Beddoes has been used. Post-stall data were derived values from report [9] which is from the wind tunnel experiments and rotor performance from stall regulated wind turbine of WEG MS-2. Apart from the aerodynamic analysis it can also do the structural dynamics, power train dynamics, closed loop control, supervisory control, modeling the wind, modeling waves and currents, modeling earthquakes and post-processing. Post-stall model from Beddos has been used. The input data required to run "GH-Bladed" for aerodynamic calculations are physical constants, airfoil sectional coefficients of lift, drag and moment, blade properties, turbine rotor and hub specifications. Steady and unsteady calculations can be carried out. Monitoring and Analysis of a Carter 200/300 wind turbine was carried out using the above program by Garrad Hassan and Partners Limited. Electro-mechanical efficiency of 90.24% at rated power was from the manufacturer of wind turbine components. The aerodynamic performance evaluation of Sangeeth wind turbine blade using "GH-Bladed " with lift and drag coefficients from NASA report[2,3,4] and post stall data from report[9] covering angle of attack ranging from –90 degrees to +90 degrees has been carried out. Figure 4.2 shows the power curve obtained from this analysis and the 10 minutes averaged field measurements. Figure 4.3 shows the coefficient of power at various tip speed ratios from GH-Bladed

5. Results and Discussion

Measured profile co-ordinates are not very accurate in view of its size and the problems associated in measurements. However blade twist arrived from the measurement and Carter 300 are in good agreement. Computation using WTPE-BEMT program it is observed that the power curve trend agree well with the field measurements up to wind velocity of 12m/s and over predicts the power beyond 12m/s. Also it is observed that the power curve shows a steep increase in power up to 15.0m/s and then rate of increase in power decreases and maintains flatness up to 24.0m/s and at higher wind speed steep increase in power. The computed cut in speed is 5.0m/s where it generates a positive aerodynamic power and measured cut in speed is very close to 5.67m/s. It can be observed from the figure 5.2 that with the assumption of total electro-mechanical efficiency of 80.36% (fairly constant in the operating range), the power curve agree very well with the field measurements even in the wind speed beyond 12m/s. It is to be noted here that the free stream velocity is assumed to be uniform along the blade span, where as in the field it varies along the span and wind velocity in the field could be highly fluctuating and non uniform. Field measured power is an 10 minutes time averaged while WTPE-BEMT is an instantaneous values. The IMPRANS

code predicted higher C_{lmax} and C_d for thickness ratios of 17% and 21%, and at the same time stall and post stall lift as well as drag coefficients in the separated regime have very high bearing on the power computed. Blade profiles twist due to aerodynamic moments and flexibility of the blade material will change the angle of attack and hence the power output change is unpredictable. Field measurement of power depends on the location, wind shear, turbulence level, dust collected on the blade over a period of time. Hence the field measured power could be as low as 15% from the steady flow calculation at wind velocity of 12m/s and 30% at wind velocity of 19m/s.This value is slightly higher than Carter observations[12]. Not much variation has been noticed at lower wind speeds.

In the "GH-Bladed" program, using the option steady calculation, predicted power curve is close to the field measurements. Power computed at rated wind speed shows slightly lower values. The power curve maintains flatness between 16m/s to 25m/s of wind velocity. This ensures the aerodynamic control of power, hence the safety of the electrical generator. Cut-in wind speed is lower than the field measurements. The power curve shows steep increase in power beyond wind speed of 25 m/s.

Conclusions

Computations of lift and drag coefficients at pre-stall, Stall and Post –Stall regimes require higher attention and accuracy, wherein power and speed (slip in electrical generator) of the turbine is controlled by stall characteristics of stall regulated turbines. Given the lower annual average wind speed of India design of a stall regulated wind turbine is a major challenging task to be accomplished. There is a scope to improve WTPE-BEMT program to get a realistic power at higher wind speeds in particularly at pre and post stall regimes. Effort is being made to get experimental results as suggested by Garrad Hassan in the post stall regime. Design data generated could be used with confidence for design of large wind turbines for Indian conditions.

Acknowledgements

The authors wish to acknowledge the support given by the M/s Sangeeth group of companies, for providing the blades and Centre for Wind Energy Technology, Chennai for providing GH-Bladed program. The authors wish to acknowledge the support given by Director, NAL and Wind Energy, Propulsion, CTFD, ESD and FRP Divisions of NAL for providing the necessary data for completing this work

References:

1) Vimala Dutta, "Implicit 2-D Navier - Stokes, solver for compressible viscous flow around airfoils". First Asian CFD conference, Hong Kong, January 16-19, 1995.

2) Robert J. Mcghee and William D. Beasley , "Low speed wind-tunnel results for a modified 13 percent thick airfoil", NASA-TM X- 74018.

3) Robert J. Mcghee and William D. Beasley , "Wind-tunnel results for a modified 17 percent thick low speed airfoil", NASA-TP- 1919.

4) Robert J. Mcghee and William D. Beasley , "Wind-tunnel results for an improved 21 percent thick low speed airfoil", NASA-TM- 78650.

5) S.J. Krishna Murthy. "Aerodynamic Analysis of Sangeeth Wind Turbine". National Aerospace Laboratories, PD-PR-0412, October 2004.

6) Garrad Hassan and Partners Limited "GH Bladed version 3.6, with theory and user manual", Vincents works, Silverthorne Lane, Bristol, England

7) Kanakmuthu et al., "Field measurement of Sangeeth wind turbine at Kethnur during April 2004 to July 2004". (Private communication) , July 2004. National Aerospace Laboratories, Bangalore.

8) Michael Antony & M. Jayaraman, R. Ravindran . "Large Wind Turbine Blade Sectional Data". (Private communication) , December, 2003. National Aerospace Laboratories, Bangalore.

9) D. C. Quarton, H. U. Schwartz and J WEI, "Monitoring and analysis of a Carter 300 wind turbine". Garrad Hassan and Partners Limited. Vincents works, Silverthorne Lane, Bristol, England.

10) Sangeeth Groups of Companies, CWT Model 300 Wind Turbine.

11) "Wind Energy Potential in Karnataka, INDIA". Renewable Energy. information from http:// www.elsevier.com/locate/renene

12) Carter. J. "Review of engineering development and performance of the lightweight Carter design from 1976". International Wind Systems. Inc. Burkburnet. TX. USA

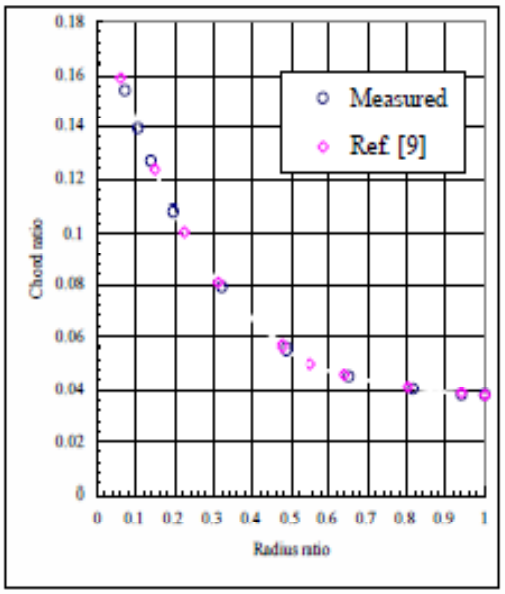

Figure 2.1 Comparison of SWT and GH Blade Chord distribution

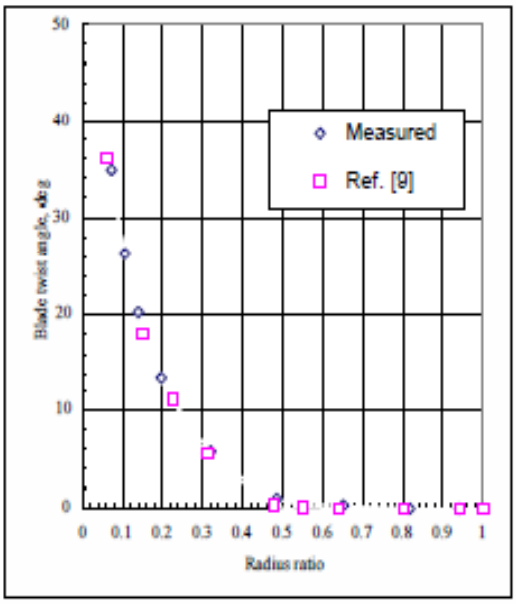

Figure 2.3 Comparison of SWT and GH Blade Twist Distribution

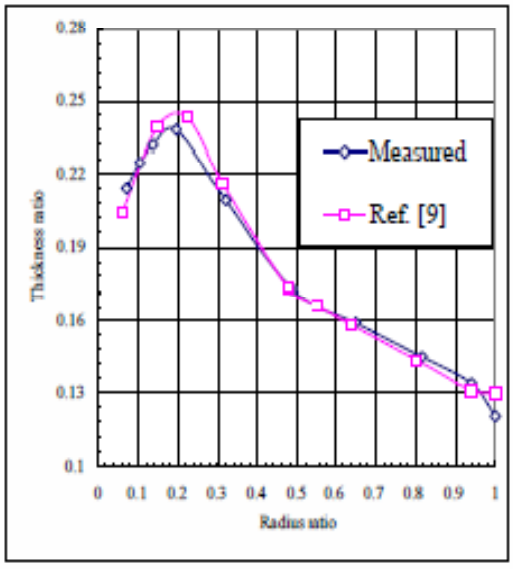

Figure 2.2 Comparison of SWT and GH Blade Thickness distribution

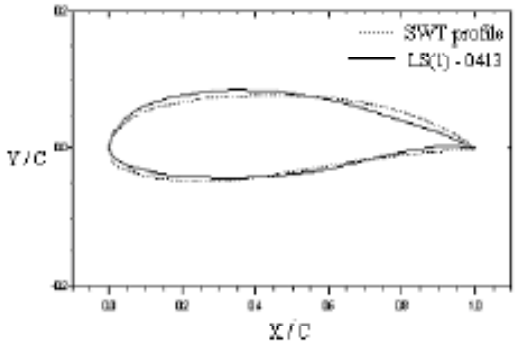

Figure 2.4 Comparison of Measured SWT and LS (1)-0413 profiles.

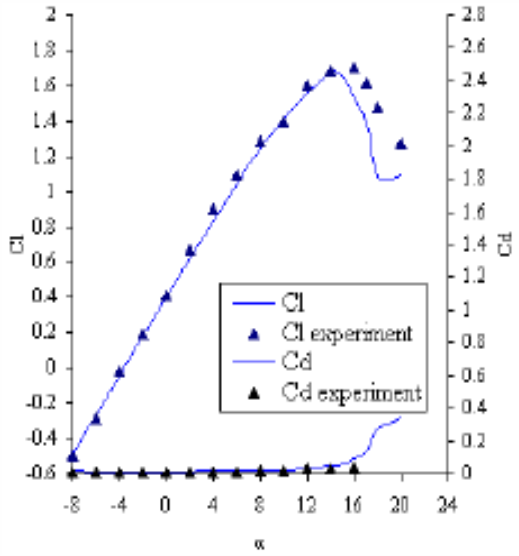

Fig 3.1a Coefficient of lift and drag
NASA LS (1) 0413
Mach = 0.15, Re = 2 million

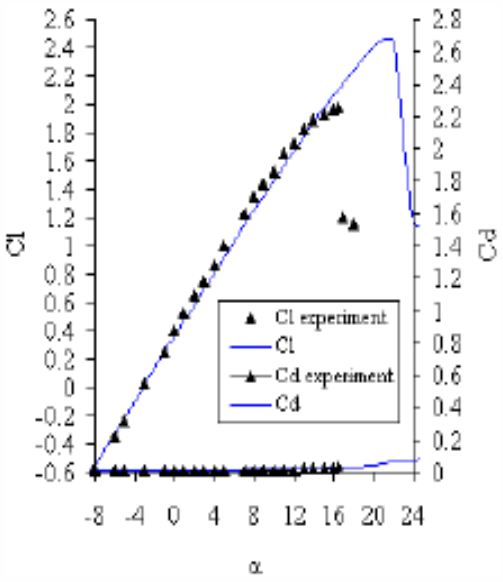

Fig 3.2a Coefficient of Lift and Drag
NASA LS (1) 0417 mod,
Mach = 0.15, Re = 4 million

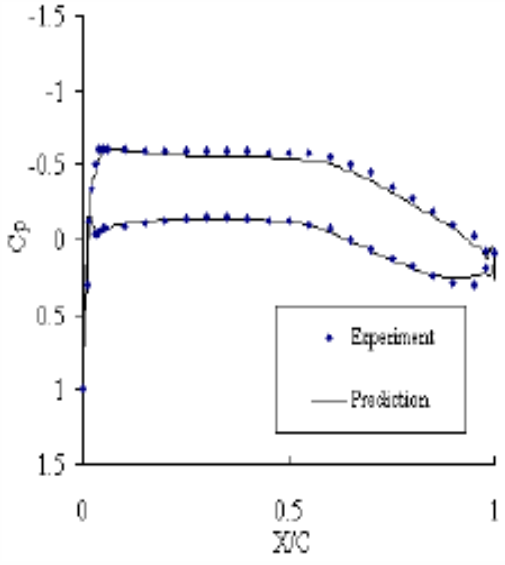

X/C
Fig 3.1b Pressure distribution of NASA
LS (1) – 0413
α = 0, Mach = 0.15, Re 2 million

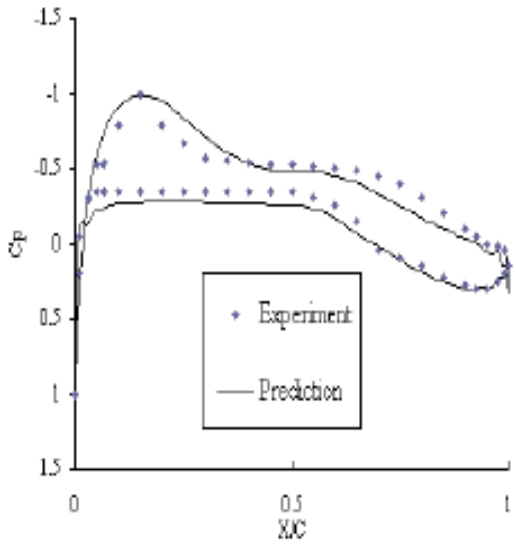

Fig 3.2b Pressure distribution of NASA
LS (1) – 0417-mod
α = 0, Mach = 0.15, Re 4 million

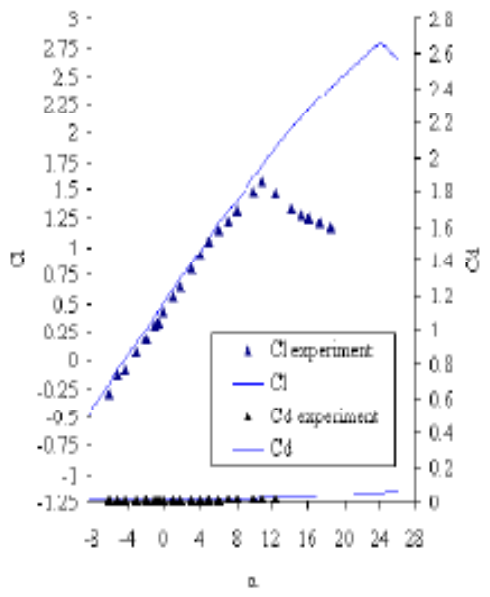

Fig 3.3a Coefficient of Lift and Drag
NASA LS (l) 0421 mod,
Mach = 0.15, Re = 4 million

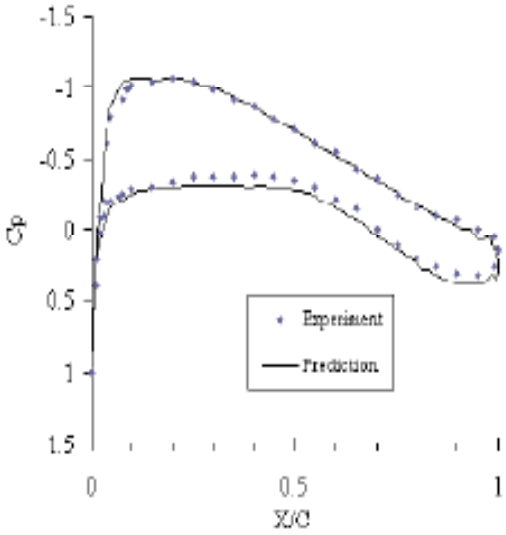

Fig 3.3b Pressure distribution of NASA
LS (1) – 0421-mod
α = 0, Mach = 0.15, Re 4 million

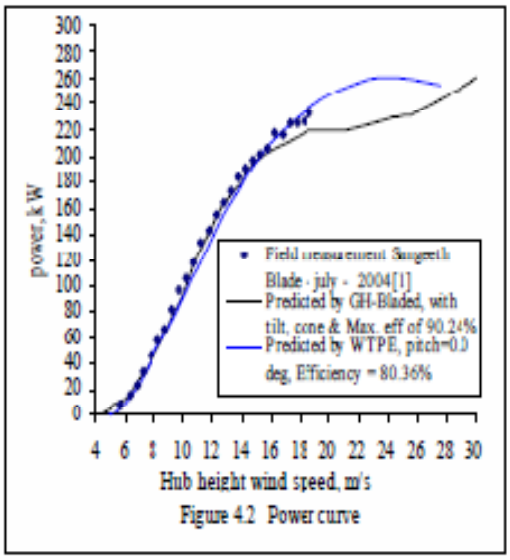

Figure 4.2 Power curve

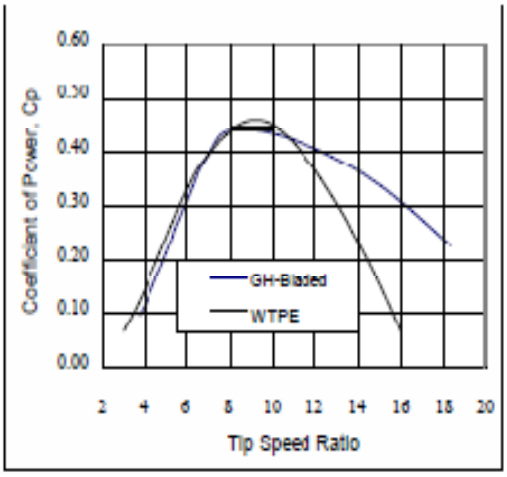

Figure 4.3 Power coefficient V/s Tip speed ratio of SWT